MOLECULAR IMAGING AND BIOLOGY

Mol Imaging Biol (2019) 21:356–367
DOI: 10.1007/s11307-018-1232-9

Published Online: 21 June 2018

RESEARCH ARTICLE

Imaging Cobalamin Uptake within Malignant Breast Tumors *In Vivo*

Douglas A. Collins

Department of Radiology, Mayo Clinic, Rochester, MN, USA

Abstract

Purpose: To image the uptake of cobalamin (Cbl) within malignant breast tumors *in vivo*.

Procedures: Prior to surgery 20 female patients with clinically suspected breast tumors were intravenously administered 0.25 μg of an In-111 labeled 5-deoxyadenosylcobalamin (AC) analog ([^{111}In]AC) and sequentially imaged with whole-body planar (WBP) and single-photon emission computed tomography (SPECT) between 2–5 h and 20–24 h post-injection (P.I.). The tumor to background (T/B) ratio for [^{111}In]AC in breast tumors at 2–5 h was correlated to its expression of estrogen (ER), progesterone (PR), and human epidermal growth factor 2 (HER2) receptors. Subsequent pulse chase (PC) experiments in nude mice burdened with the MDA-MB-231 triple-negative (TN) breast tumor xenograft measured the effect that pulses of AC or dexamethasone (DEX) had on [^{111}In]AC uptake in both normal murine tissue and the TN breast tumor.

Results: The mean [^{111}In]AC T/B ratio of the patients' 18 resected tumors was 5.8. Comparing ER- and PR-positive tumors ($n = 11$) to TN and HER2-positive tumors ($n = 7$), the mean [^{111}In]AC T/B ratios at 2–5 h P.I. were 3.2 (range 1.8–5.6) and 10.4 (range 3.3–22.5), respectively. Pulses of 2.0 μg of AC at 2, 8, or 24 h; or 40.0 μg of DEX at 24 h prior to injecting 0.5 μg of [^{111}In]AC, increased mean tracer uptake in the MDA-MB-231 tumors by 26.4, 71.5, 92.6, and 49.1 %, respectively. Only the 2- and 24-h PC intervals concomitantly suppressed [^{111}In]AC uptake in normal murine tissue while enhancing [^{111}In]AC uptake in MDA-MB-231 tumors.

Conclusion: The uptake of Cbl within malignant breast tumors can be imaged clinically. Cbl uptake is greatest in TN and HER2-positive breast tumors. A solitary bolus of AC or DEX increases the [^{111}In]AC uptake within a breast tumor *in vivo*. Investigating the cytogenetic mechanisms controlling the endocytosis of Cbl in malignant breast tumors is warranted.

Key words: Breast cancer, Cobalamin metabolism, Receptor imaging, Transport proteins, Genes

Introduction

The annual screening of women with mammography has contributed to the overall reduction in breast cancer mortality by increasing the early detection of clinically occult non-palpable breast tumors [1]. Depending upon a woman's ethnicity and breast tissue density, approximately 5 to 20 % of breast tumors evade mammographic detection and clinically present as a palpable mass or metastatic lesion [2, 3].

Since the genetic and biochemical transformations occurring within a breast tumor ultimately construct the anatomic abnormalities perceived on mammography, molecular breast imaging (MBI) has gradually developed into a clinical tool capable of detecting aberrant metabolism within small

Electronic supplementary material The online version of this article (https://doi.org/10.1007/s11307-018-1232-9) contains supplementary material, which is available to authorized users.

Correspondence to: Douglas Collins; *e-mail:* collins.douglas@mayo.edu

malignant breast tumors [4]. The instrumentation of MBI, which includes positron emission mammography (PEM), single-photon mammography (SPM), and positron emission tomography/X-ray computed tomography (PET/CT), and the employment of these modalities in imaging the uptake of various metabolic tracers within breast tumors was recently reviewed [5, 6].

As a supplemental screening exam, both PEM and SPM have become effective tools in discovering mammographically and clinically occult non-palpable breast tumors in women with dense breast tissue [7]. If MBI is to ultimately function as a primary screening modality for pinpointing the early biochemical changes arising within an occult breast cancer, it must be paired with plasma and/or urine biomarkers indicating a metabolic pathway amenable to clinical imaging is aberrantly upregulated within a malignant breast tumor [8].

The cobalamin (Cbl or vitamin B12) metabolic pathway was initially observed to be upregulated in mammary carcinomas shortly after the vitamin was discovered in 1948 [9]. Two of the proteins within the Cbl metabolic pathway were eventually found to be elevated in the serum of breast cancer patients [10, 11]. Cbl was ultimately discovered to have two co-enzymatic functions that uniquely support cellular proliferation. Within the cytoplasm, methylcobalamin (MC) is the co-enzyme for methionine synthase (MS). MS directly or indirectly supports cellular production of methionine, thymidine, and S-adenosylmethionine to sustain protein anabolism, DNA synthesis, and numerous methylation reactions, respectively. In the mitochondria, 5′-deoxyadenosylcobalamin (AC) is the co-enzyme for methylmalonyl CoA mutase (MMCM). MMCM represents the final step in the catabolism of branched chain amino acids, odd chain fatty acids, and cholesterol. The end product succinyl-CoA supports energy production (ATP) and tetrapyrrole ring synthesis.

The increased uptake of Cbl within rapidly proliferating cells was initially depicted diffusely throughout fetal murine tissue *in utero* and selectively in transplanted mammary tumors in adult mice by Co-57 labeled cyanocobalamin (CC) or [^{57}Co]CC (Fig. 1) and time-dependent autoradiography [12]. [^{57}Co]CC additionally assisted in deciphering that transcobalamin (TC) was the sole transport protein in serum to selectively bind and deliver Cbl to every tissue type in humans, that holo-TC (TC carrying a single molecule of Cbl) underwent endocytosis by the dedicated transcobalamin receptor (TC-R) expressed on all human cell membranes [13], that holo-TC was primarily saturated with AC [14], and that AC was the major co-enzymatic form of Cbl (50–70 %) in both normal and malignant human cells [15].

The upregulated expression of TC-R on tumor cell membranes, in association with a greater cytoplasmic concentration of [^{57}Co]CC bound to TC during DNA replication, initially established that the TC:TC-R pathway was the primary mechanism responsible for Cbl endocytosis in malignant tissue [16]. To directly investigate Cbl uptake in tumors by the TC:TC-R pathway, we previously described the synthesis and radiolabeling of an AC analog [17]. *In vitro* we demonstrated that both TC and intrinsic factor (IF), the Cbl transport protein uniquely secreted by gastric parietal cells to capture newly ingested Cbl in the proximal small bowel and deliver it to the cubilin-amnionless (CUBAM) receptors expressed in the terminal ileum, both selectively bound and transported [^{111}In]AC. *In vivo* [^{111}In]AC scintigraphically depicted the increased uptake of Cbl within transplanted human tumor xenografts in nude mice [17, 18], in naturally occurring feline and canine tumors diagnosed by veterinarians [18, 19] and in a variety of clinically suspected malignancies in patients [20–22].

Here an In-111 radiolabeled AC analog or [^{111}In]AC (Fig. 1) was clinically employed to depict the uptake of Cbl within suspected breast tumors in 20 female patients. The tumor to background (T/B) ratio for [^{111}In]AC in breast tumor was correlated to its expression of estrogen (ER), progesterone (PR), and human epidermal growth factor 2 (HER2) receptors. Subsequent dose escalation (DE) and pulse-chase (PC) experiments were pursued in nude mice burdened with the human triple-negative (TN) breast tumor xenograft MDA-MB-231 to investigate our clinical observation of greater [^{111}In]AC uptake in the tumors of patients ingesting Cbl or dexamethasone (DEX) 24 h prior to [^{111}In]AC administration [20, 21].

Summarized within is the [^{111}In]AC human and murine breast tumor imaging data, prior comparative investigations into Cbl uptake within normal and malignant breast tissue, and initial inquiry into potential genetic perturbations influencing the expression of the three Cbl transport proteins (transcobalamin, intrinsic factor, haptocorrin) and five Cbl receptor proteins (transcobalamin-R, megalin, cubilin, amnionless, asialoglycoprotein-R) within breast tumors.

Materials and Methods

[^{111}In]AC Human Biodistribution Study

The human [^{111}In]AC biodistribution study was approved by the Institutional Review Board at Mayo Clinic and the Federal Drug Administration and executed in accordance with the ethical standards delineated in the 1964 Helsinki Declaration. Informed consent was obtained from all individual participants prior to entering the study. A total of 20 female patients with clinically palpable or suspected underlying breast malignancies were enrolled from 1999 to 2005.

Prior to the intravenous (I.V.) administration of [^{111}In]AC, a 5 ml venous blood sample was acquired from all patients to establish a baseline Cbl plasma concentration. A maximum dose of 650 μCi of [^{111}In]AC was administered. The [^{111}In] radiolabeling of the AC analog, calibration of the [^{111}In]AC dose syringe prior to and after I.V. administration, the [^{111}In]AC serum $T_{1/2}$

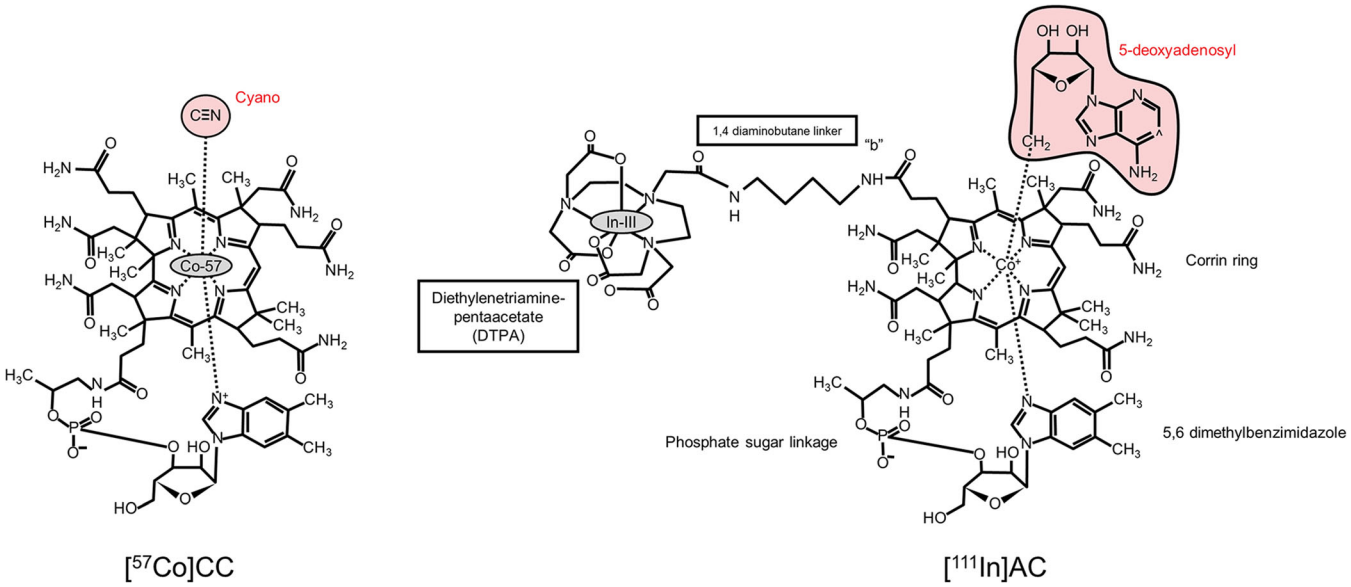

Co-enzyme forms of Cbl	Cbl-dependent enzymes
5-deoxyadenosylcobalamin (AC)	Methylmalonyl-CoA-mutase (MMCM)
Methylcobalamin (MC)	Methionine synthase (MS)
Cbl transport proteins	**Cbl cell membrane receptor proteins**
Transcobalamin (TC)	Transcobalamin (TC-R)
Intrinsic factor (IF)	Megalin (MEG)
Haptocorrin (HC)	Cubilin-amnionless (CUBAM)
	Asialoglycoprotein receptor (ASGP-R)

Fig. 1. Molecular structures of In-111-labeled 5-deoxyadenosylcobalamin ([^{111}In]AC) and Co-57-labeled cyanocobalamin ([^{57}Co]CC). Above the corrin ring are the β-ligands (5-deoxyadenosyl and cyano). Below is the α-ligand 5,6 dimethylbenzimidazole (DMB) and the phosphate sugar that links DMB to the corrin ring. Summary of the biochemical names and abbreviations for the co-enzymatic forms of cobalamin (Cbl), Cbl-dependent enzymes, and dedicated Cbl transport and receptor proteins.

clearance assay, quantification of urinary excretion of [^{111}In]AC, and the acquisition of the whole-body planar (WBP) and single-photon emission computed tomographic (SPECT) images were performed as previously described [20, 21].

All patients were imaged prior to biopsy or breast surgery. The [^{111}In]AC T/B ratio of a breast lesion was calculated from the earliest acquired SPECT images (range 2–5 h). Specifically, on coronal SPECT images, the [^{111}In]AC activity (counts per min or CPM) in a breast tumors region of interest (ROI) was divided by the [^{111}In]AC activity from an ROI of normal breast tissue located in a correlative anatomic location of the contralateral breast. An [^{111}In]AC T/B ratio of 2.0 or greater was applied to delineate malignant from benign breast tissue [23, 24]. A breast tumor [^{111}In]AC T/B ratio was correlated to its reported expression of ER, PR, and HER2 receptors on post-surgical pathology.

[^{111}In]AC Murine DE and PC Experiments

The Institutional Use and Animal Care Committee at Mayo Clinic approved the murine [^{111}In]AC DE and PC experiments. All applicable national guidelines for the care and use of animals were followed. Female nude mice (8–12 weeks old, 20–25 g) were inoculated with 1×10^6 MDA-MB-231 breast cancer cells in the dorsal cervical soft tissue. Once tumors reached 1.0 cm in size, mice in groups of five were studied per dose or time interval. A dose of [^{111}In]AC was injected *via* the intra-peritoneal (I.P.) route utilizing an insulin syringe with a 27-g needle. The [^{111}In]AC DE experiments were pursued prior to the PC experiments to approximate the dose that the AC tracer would competitively inhibit its own uptake in normal murine tissue.

The DE experiments evaluated I.P. injections of 0.1 μg (240 μCi), 0.5 μg (1200 μCi), or 1.0 μg (2400 μCi) of [^{111}In]AC (1.58 μg of AC = 1 nmole of AC). The PC

experiments consisted of an initial I.P. pulse dose of 2.0 μg of AC or 40 μg DEX at 2, 8, or 24 h followed by an I.P. chase dose of 0.5 μg [^{111}In]AC. All mice were euthanized by carbon dioxide asphyxiation at 24 h post [^{111}In]AC injection and immediately imaged on a clinical gamma camera (General Electric) with medium energy collimators. Normal tissue (brain, lung, heart, liver, spleen, left kidney, left quadriceps, left flank fat) and the MDA-MB-231 tumors were harvested and assayed for counts/min/mg tissue (CPM/mg) after the completion of imaging on all DE and PC experiments as previously described [17].

Results

Imaging Cbl Uptake within Patient Breast Tumors

All 20 women enrolled were Caucasian. Mean weight and age of the patients were 75.6 kg (range 58–103 kg) and 53.9 years (range 35–80 years), respectively. The mean Cbl plasma concentration was 595 ng/l (range 70–2000 ng/l). Normal range is 180–914 ng/l. The mean injected dose of [^{111}In]AC per patient was 600 μCi (range 420–650 μCi) or ~0.25 μg of the AC analog. Previously this was incorrectly reported as 2.2 μg of AC analog [20, 21]. The error in dilution of the vials containing the AC analog was discovered during the [^{111}In] radiolabeling for the murine experiments. Serum $T_{1/2}$ clearance was unchanged at 6.9 min. Mean 24 h urinary excretion of [^{111}In]AC was 28 % (range 13–42 %).

Of the 20 patients enrolled, one patient (d/h) was imaged and biopsied twice; initially prior to right mastectomy and 2 years post-mastectomy secondary to the development of new palpable metastatic disease. Therefore, a total of 21 suspicious breast lesions were investigated in 20 patients. The biodistribution of [^{111}In]AC is depicted in 14 of the women enrolled (Figs. 2, 3, and 4). Of the 21 suspicious breast lesions, 18 were malignant and 3 were benign (Table 1). Although both the WBP and SPECT images at 2–5 h depicted [^{111}In]AC uptake in 94.4 % (17/18) of the suspected breast tumors, smaller breast tumors (0.7–1.0 cm) were better defined by SPECT. The WBP and SPECT images at 20–24 h did not improve the breast tumor T/B for [^{111}In]AC (not shown).

The mean [^{111}In]AC T/B ratio of the 18 surgically resected malignant breast tumors was 5.8 (range 1.8–22.5). The [^{111}In]AC avid breast tumors were predominantly of high nuclear grade, invasive ductal carcinomas (IDC). However, [^{111}In]AC uptake was imaged within foci of high-grade ductal carcinoma *in situ* (DCIS), invasive lobular carcinoma, and an inflammatory breast cancer. Contrasting the uptake of [^{111}In]AC in aggressive TN and HER2 receptor-positive tumors (patients d, e, f, h, i, l, q; $n = 7$) to ER- and PR-positive tumors (patients c, g, j, k, m, n, o, p, r, s, t; $n = 11$), the mean T/B ratios were 10.4 (range 3.3–22.5) and 3.2 (range 1.8–5.6), respectively.

Excluding one patient with a large 7.5-cm breast tumor and three diffuse segmental breast cancers, the average size of the [^{111}In]AC avid breast tumors was 1.9 cm (range 0.7–3.4 cm). The majority of patients with [^{111}In]AC avid breast tumors (12/17) had not ingested Cbl or DEX 24 h prior to tracer administration. In this group of patients, the mean T/B ratio was 3.5 (range 2.0–5.6) with a mean Cbl plasma concentration of 428 (range 70–580 ng/l). In the remainder of patients (5/17) with [^{111}In]AC avid breast tumors that had ingested Cbl or DEX 24 h prior to [^{111}In]AC injection, the mean T/B ratio was 12.9 (range 5.9–22.5) with a mean Cbl plasma concentration of 1150 (range 710–2000 ng/l).

The one patient imaged twice was within this subgroup (d, f, h, i, q). Her TN breast tumor was associated with the greatest volume of metastatic disease, the two highest serum concentrations of Cbl, the two greatest [^{111}In]AC T/B ratios, and the most urinary excretion of tracer (42 %) at 24 h. Conversely, in the three true negative (TN) scans, and the one false negative (FN) scan (patient t), the [^{111}In]AC T/B ratios were 1.3 (range 1.0–1.5) and 1.8, respectively. Mean Cbl plasma concentration in those four patients (3 TN + 1 FN) was 402 (range 350–488 ng/l).

Two patients (m, n) had [^{111}In]AC avid metastatic foci of breast tumor to the brain and retroperitoneal lymph nodes, respectively. Intriguingly, the [^{111}In]AC T/B ratios in the metastatic lesions of patients m and n were 5.8 and 6.9, respectively, compared to 2.8 and 3.2 in their primary breast tumors. In the only two patients (f, n) undergoing both [^{111}In]AC SPECT and 2-deoxy-2-[^{18}F]fluoro-D-glucose ([^{18}F]FDG) PET/CT imaging, the uptake of [^{111}In]AC and [^{18}F]FDG in the primary and metastatic foci of breast tumor were visually congruent despite injecting 0.6 mCi of [^{111}In]AC compared to 15.2 mCi of [^{18}F]FDG.

Murine DE and PC Data

Neither the 0.1 or 0.5 μg bolus of [^{111}In]AC (twice the dose administered to patients) saturated [^{111}In]AC uptake in normal murine tissue or the MDA-MB-321 tumors. A 1.0 μg bolus of [^{111}In]AC partially suppressed its own uptake in normal tissue (excluding the kidneys and lungs), while increasing mean [^{111}In]AC activity in the MDA-MB-231 tumors by 35.1 % (Table 2).

A 24-h PC interval between AC and [^{111}In]AC injections caused the greatest mean increase in [^{111}In]AC activity in the MDA-MB-231 tumors (92.6 %). A 24-h PC interval between DEX and [^{111}In]AC injections increased mean MDA-MB-231 tumor activity by 49.1 %. On both the AC and DEX 24-h PC intervals, the [^{111}In]AC activity in renal tissue increased ~3.5 and 4.3 times, respectively. [^{111}In]AC uptake in the

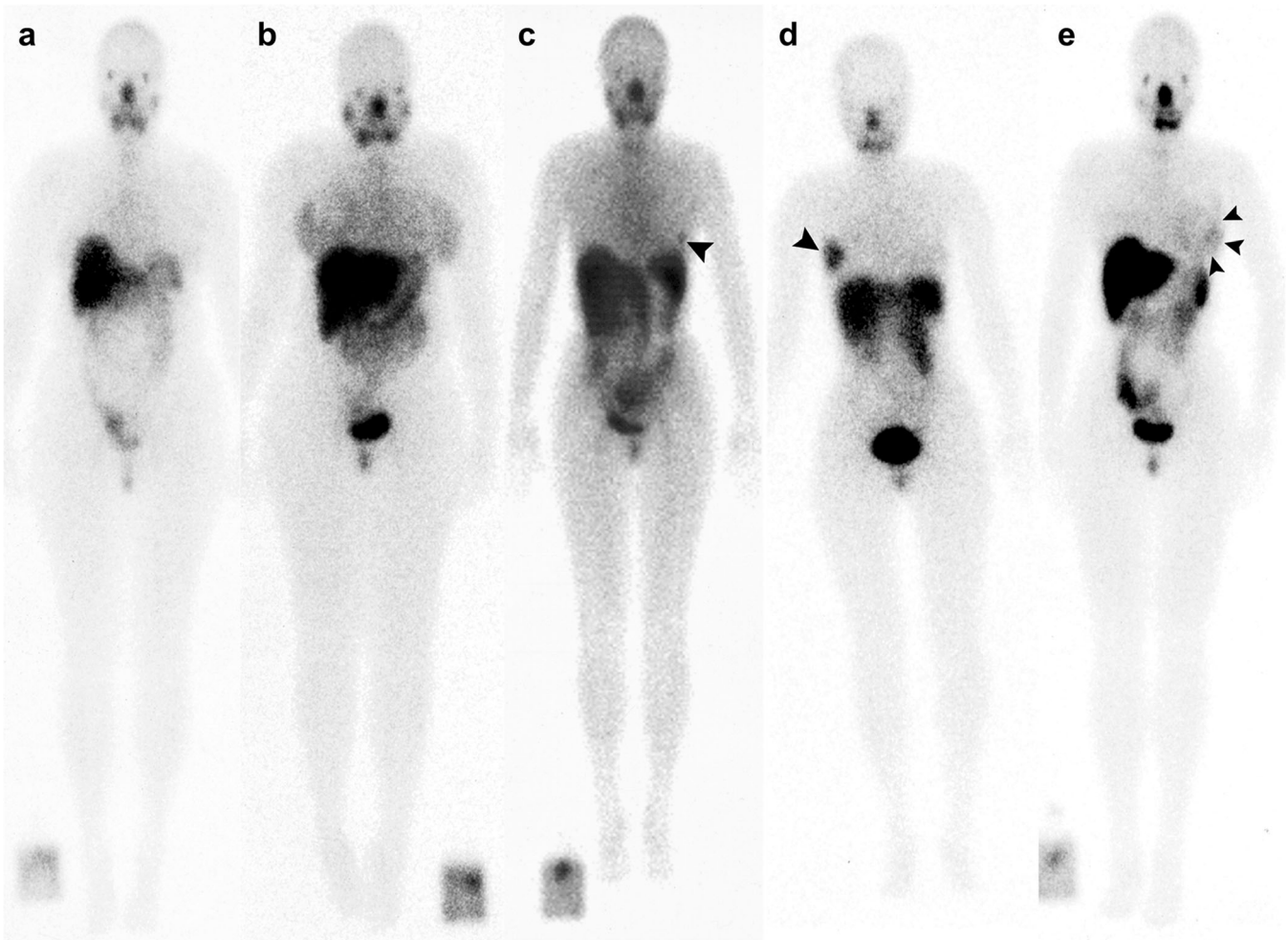

Fig. 2. **a** Patient 2 years post-resection of an invasive ductal breast cancer in the upper outer quadrant of the right breast. New palpable mass noted immediately superior to the surgical scar. No focal [^{111}In]AC activity within the breasts or axillae. **b** The only patient with bilaterally diffuse [^{111}In]AC activity in the breasts. The clinically large palpable mass in the right upper breast is photopenic with a mild rim of increased [^{111}In]AC activity. **c** Small 1.6 cm left breast cancer (black arrowhead) in the lower outer quadrant (4). **d** Large 7.5 cm right breast cancer (black arrowhead). The image was acquired at 0.5 h post [^{111}In]AC administration. **e** Diffuse [^{111}In]AC uptake in an inflammatory breast cancer involving the inferolateral left breast (three black arrowheads).

remainder of normal tissue was either not significantly changed or mildly suppressed.

Only the AC 2-h PC interval suppressed mean [^{111}In]AC activity in all normal tissue (excluding the kidneys), while concomitantly increasing mean [^{111}In]AC activity in the MDA-MB-231 tumors by 26.4 % (Table 2). Conversely, the AC 8-h PC interval uniquely caused the greatest mean increase in [^{111}In]AC activity in the majority of normal tissue (kidney, liver, fat, lung, skeletal muscle) and the second greatest mean increase of [^{111}In]AC activity (71.5 %) in the MDA-MB-231 tumors.

The trend of greatest to least [^{111}In]AC avid tissue on the DE and PC experiments was consistently renal> tumor> liver> fat> lung> spleen> heart> muscle> brain. However, on the *post mortem* WBP images, only the kidneys, MDA-MB-231 breast tumors and liver demonstrated any discernable [^{111}In]AC activity (Fig. 5).

Discussion

Reported here is the largest cohort of female patients to have had Cbl uptake scintigraphically depicted within clinically suspected breast malignancies prior to surgery. The mean uptake of [^{111}In]AC in the 18 resected breast tumors was 5.8 times greater than in normal breast tissue. Although the limited number and bias selection of patients restricts any statistical conclusions, a pattern of [^{111}In]AC uptake was observed in the foci of suspected breast tumor.

First, the mean [^{111}In]AC T/B ratios were greater in biologically aggressive TN and HER2-positive breast tumors

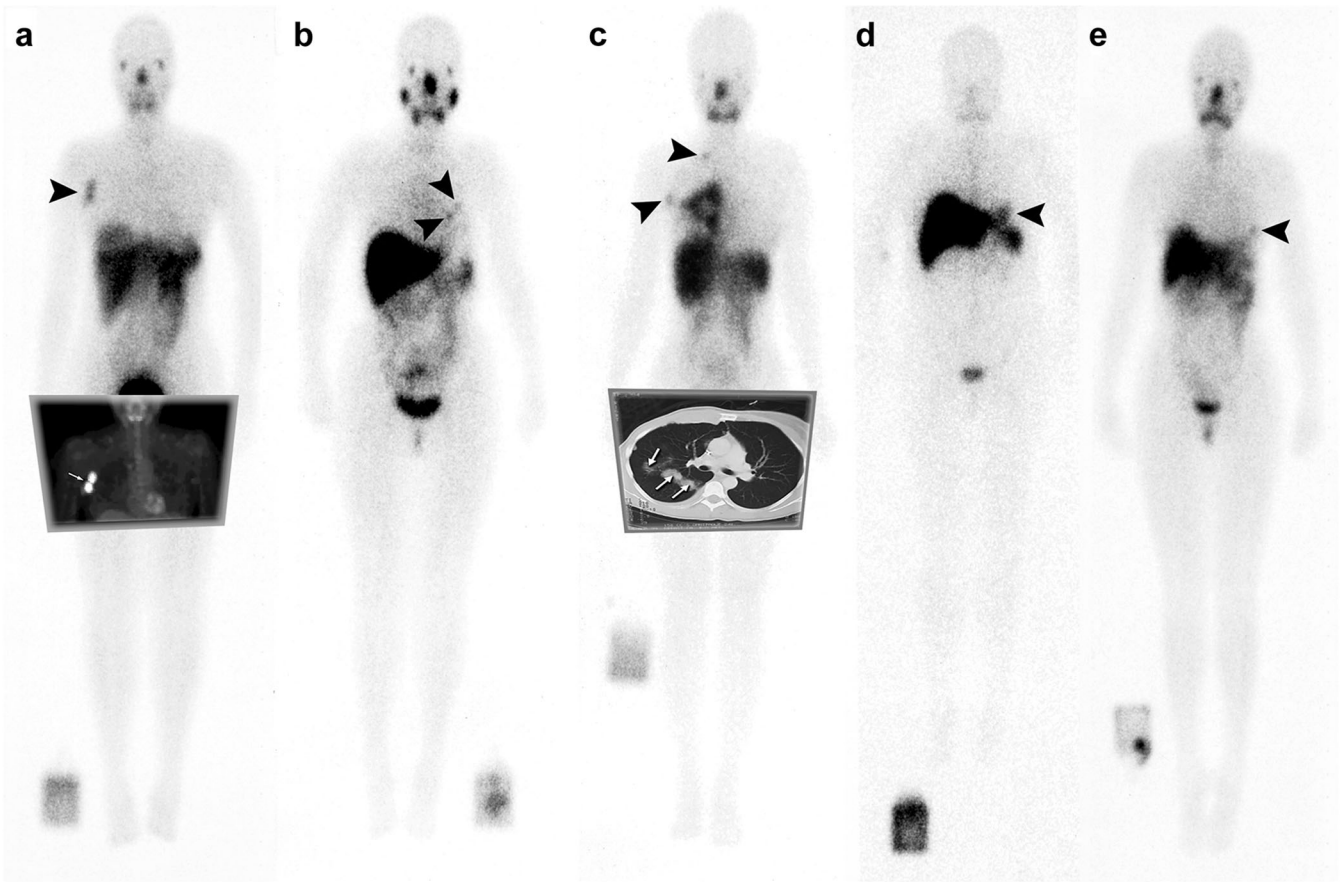

Fig. 3. **a** Focal [^{111}In]AC activity in a right breast tumor and axillary lymph nodes (black arrow head). Corresponding [^{18}F]FDG activity in the tumor and nodes on the inset [^{18}F]FDG MIP image (white arrow). **b** Multifocal left breast cancer (black arrowheads) delineate two (0.7 and 0.9 cm) of the three foci in the upper inner quadrant. A third focus was depicted by SPECT. **c** Two years after right mastectomy patient d returns with new metastatic right supraclavicular and right axillary lymph nodes (black arrowheads). White arrows on the inset CT point to three of the multiple [^{111}In]AC avid pulmonary nodules in the right lung. **d** A 3.4 cm breast cancer in the inferomedial left breast (black arrowhead). **e** Small 0.9 cm left breast cancer in the lower outer quadrant (black arrowhead).

compared to ER- and PR-positive tumors. Second, metastatic foci of breast cancer could have greater [^{111}In]AC T/B ratios than their primary breast tumor. Third, the greatest [^{111}In]AC T/B ratios occurred in the breast tumors of patients with the highest serum concentrations of Cbl. This counterintuitive finding correlated to a patient's ingestion of Cbl or DEX 24 h prior to [^{111}In]AC administration.

The murine 24-h PC experiments confirmed the latter observation. The human and murine [^{111}In]AC imaging data additionally indicates that the capacitance for Cbl uptake in malignant breast tumors and normal tissue is differentially robust. Specifically, the recommended daily allowance (RDA) for Cbl in humans and mice is 2.4 and 0.1 μg, respectively [25, 26]. With patients excreting an average of 28 % of the 0.25 μg dose of [^{111}In]AC into urine over a 24-h interval, it was postulated that [^{111}In]AC uptake would rapidly become saturated in normal murine tissue and the MDA-MB-231 tumors.

However, partial saturation of [^{111}In]AC uptake in normal murine tissue (excluding the kidneys and lungs) did not significantly occur until the 1.0 μg bolus of [^{111}In]AC. Even at that dose, which was four times the dose administered to patients and 10 times the murine RDA, no organ or tissue type was saturated greater than 67 %. That occurred in brain tissue. Conversely, [^{111}In]AC uptake in the MDA-MB-231 tumors and murine kidneys never reached saturation on either the DE or PC experiments.

Patient d/h underscores the robust nature of Cbl uptake in an aggressive TN breast tumor. Her unique ingestion of supraphysiologic doses of vitamins as a sole therapeutic regimen, including 2000–5000 μg of Cbl/day, both multiple years prior to and in between her two episodes of [^{111}In]AC imaging, was associated with the highest [^{111}In]AC T/B ratios and two greatest concentrations of Cbl in serum.

Intriguingly, hepatic uptake of [^{111}In]AC in patient d/h, the primary site of Cbl storage in humans, was not suppressed compared to the cohort. The finding indicates

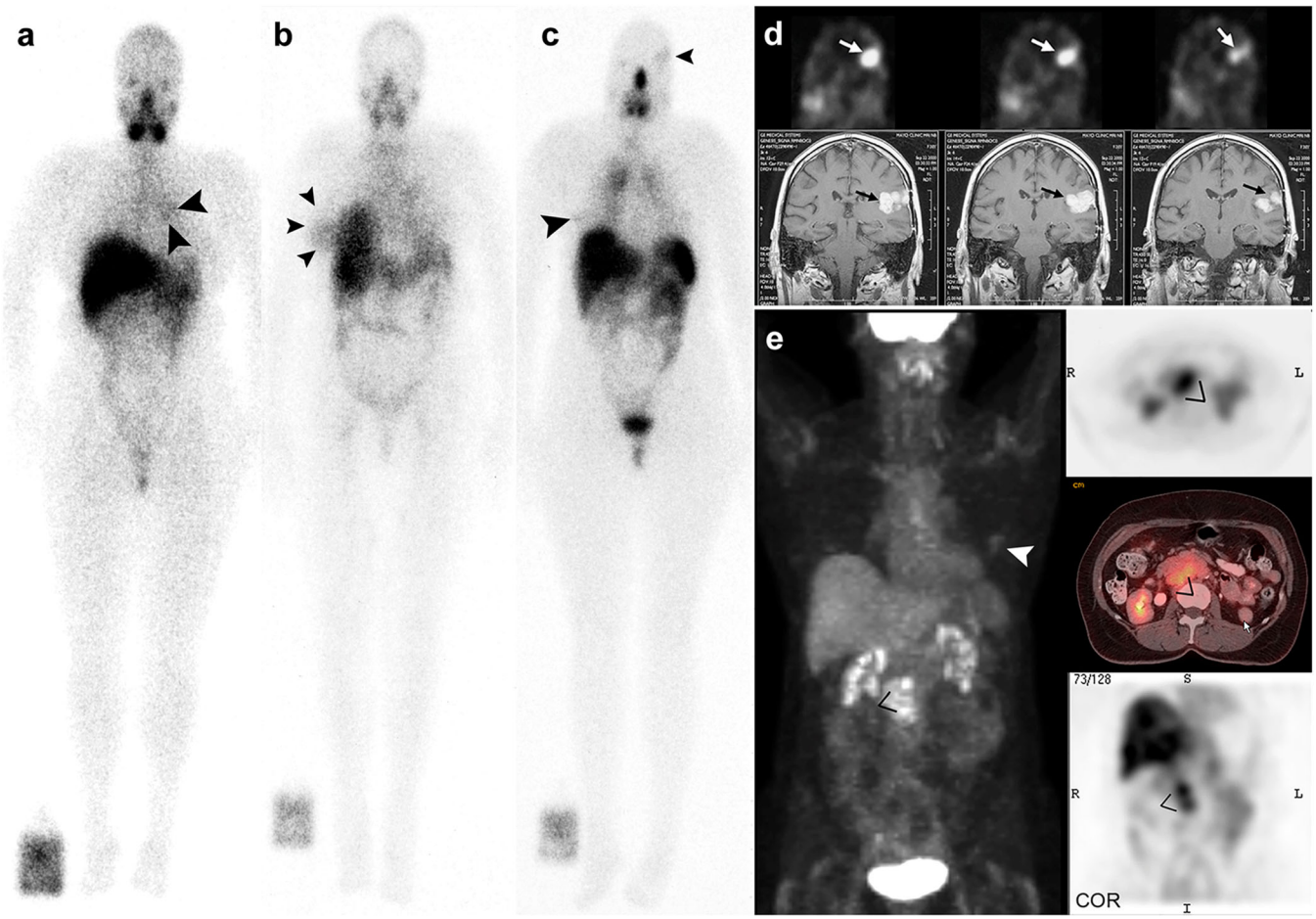

Fig. 4. **a** Small 1.2 cm left breast cancer in the upper inner quadrant (superior black arrow head). Increased background activity in the left hilum (inferior black arrowhead). **b** Diffuse [^{111}In]AC activity in the inferolateral right breast (three black arrowheads) corresponds to diffuse, multisegmental microcalcifications of invasive DCIS. Faint diffuse symmetric mediastinal activity (not delineated). **c** A small 0.7 cm right breast cancer (black arrowhead). Incidental diffuse bilateral hilar mediastinal [^{111}In]AC activity. Focus of [^{111}In]AC activity in the brain on the WBP images (black arrowhead) corresponds to **d** the adjacent three SPECT coronal images with metastatic breast cancer in the left cerebral hemisphere (white arrows). Immediately below are correlative coronal MRI images depicting the gadolinium enhancing metastatic breast tumor (black arrows). **e** The breast tumor (white arrowhead) on the MIP [^{18}F]FDG images is less metabolically active than the retroperitoneal metastatic nodal disease (black "V" marker). Corresponding [^{111}In]AC coronal (COR) images with comparable activity in the retroperitoneal metastatic nodes (black "V" marker). Transaxial slice of the retroperitoneal nodal disease (black "V" marker) on both the colored [^{18}F]FDG PET/CT and the black and white [^{111}In]AC SPECT images.

that the capacitance for Cbl uptake in her liver and foci of primary and metastatic breast tumor were not saturated. Correspondingly, neither the MDA-MB-231 tumors or murine kidneys, the primary site of Cbl storage in mice, were saturated by the large doses of AC or [^{111}In]AC.

Potential PC Mechanisms Impacting Cbl Uptake in Breast Tumors

A recent study observed that patients with chronic excess Cbl supplementation had the highest serum concentrations of holo-TC and sCD320 (the extracellular soluble component of TC-R). This subgroup of patients had Cbl serum levels greater than 1000 pmol/l [27]. It was posited that this subgroup of patients had developed an underlying increase in cellular metabolism and cell membrane TC-R activity that initiated an excess release of TC and sCD320 into the intravascular space.

The hypothesis may partially explain the elevated Cbl serum concentrations and greater breast tumor [^{111}In]AC T/B ratios in the Cbl-supplemented patients. The findings imply that Cbl supplementation increased the endocytosis of [^{111}In]AC by upregulating TC-R expression on the cell membranes of a breast tumor. Conversely, the decreased [^{111}In]AC activity in patient d/h lacrimal and salivary glands may exemplify how the chronic ingestion of Cbl suppresses its own uptake in normal tissue.

Table 1. Patient [^{111}In]AC breast tumor imaging data and correlative pathology

ID	Age	Cbl	Image	T/B	NG	IG	ER	PR	HR	Surgical pathology
a	70	423	TN	1.0						Benign hamartoma, 1.8 × 1.5 × 0.6 cm right mass
b	36	488	TN	1.5						Ductal ectasia with periductal mastitis
c	59	491	TP	3.9	2/3	3/4	+	+	–	IDC, 1.6 × 1.3 × 1.1 cm left breast mass, LN
d	44	1278	TP	22.5	2/3	3/4	–	–	–	IDC, 7.5 cm fungating right breast mass, LN+
e	75	379	TP	3.3	2/3	3/4	+	–	+	Diffuse left inflammatory breast cancer, LN–
f	41	721	TP	5.9	3/3	4/4	–	–	–	Right axillary tail mass 3.0 × 2.4 × 1.7 cm LN+
g	58	420	TP	3.9	2/3	2/4	+	+		IDC 0.7 and 0.9 cm solid papillary, LN–
h	46	2000	TP	14.8	3/3	4/4	–	–	–	Poorly differentiated metastatic breast, 2.1 cm LN+
i	35	710	TP	12.7	2/3	4/4	–	–	–	IDC, 3.4 × 3.0 × 2.8 cm left breast mass, LN+
j	48	575	TP	3.4	2/3	2/4	+	+	–	IDC, 0.9 cm left breast mass, LN–
k	35	580	TP	2.5	2/3	2/4	+	+	–	DCIS, comedo type, 1.2 cm left breast, LN–
l	75	361	TP	5.2	2/3	4/4	–	–	+	Segmental DCIS calcifications, LN–
m	48	575	TP	2.8	2/3	3/4	+	+	–	IDC, 0.7 cm right breast mass, left brain mets, LN–
n	59	352	TP	3.2	2/3	3/4	+	+		IDC, 1.8 × 1.6 cm right breast mass, LN–
o	60	437	TP	2.0	3/3	4/4	–	–		IDC, 0.8 cm mass in LUOQ, 15/22 LN+,
p	39	503	TP	5.6	2/3	3/4	+	+	–	IDC, 1.9 × 1.5 × 1.2 cm LN+
q	44	1041	TP	8.4	3/3	4/4	+	–	+	IDC, 3.6 × 3.4 × 1.9 cm, LN+
r	53	396	TP	3.5	2/3	3/4	+	+		Mixed lobular and ductal 1.2 × 1.1 × 0.7 cm, LN–
s	58	70	TP	2.1	II	4/4	+	+	–	Segmental invasive lobular CA, LN–
t	71	350	FN	1.8	1/3	1/4	+	+		DCA tubular type, 0.9 cm mass, LN–
u	63	347	TN	1.0						Fibrosis and giant cell reactions

Cbl cobalamin plasma concentration, *TP* true positive, *TN* true negative, *FN* false negative, *T/B* tumor to background ratio, *NG* nuclear grade, *IG* invasive grade, *Breast tumor expression of ER* estrogen receptor, *PR* progesterone receptor, *HR* human epidermal growth factor 2 receptor, *Positive* (+), *Negative* (–), *Borderline* (–), *IDC* intraductal carcinoma, *DCIS* ductal carcinoma *in situ*, *DCA* ductal cancer, *LN* axillary lymph node status for metastasis

Specifically, in mice subcutaneously administered 2.37 μg of CC/h for 4 weeks, a 50 % reduction in both TC and TC-R transcription, and Cbl concentration occurred in the lacrimal and salivary glands [28]. It is reasonable to posit that the chronic ingestion of Cbl reduced [^{111}In]AC uptake in the majority of patient d/h normal tissue and contributed to increasing her [^{111}In]AC T/B ratios and urinary excretion of tracer.

Precisely how a solitary bolus of AC or DEX enhanced [^{111}In]AC uptake in the MDA-MB-231 and patients breast tumors remains to be determined. Nevertheless, two prior human studies and the current murine 8 h PC data indicate that the TC:TC-R pathway was acutely upregulated. Specifically, in patients given a solitary I.V. bolus of 0.2 μg of CC/kg, the mean TC serum concentration was suppressed by 53.5 % at 0.5 h post-injection, but gradually approached normal pre-injection levels by 8 h [29].

Correspondingly, female patients administered a single intramuscular injection of 120 mg of DEX for two consecutive days had a mean 59 % increase in TC serum concentration [30]. These studies imply that a large bolus of Cbl or DEX acutely triggers a cellular or endovascular release of apo-TC. Given that the $T_{1/2}$ of TC-R renewal on cell membranes is 8 h, the murine 8 h PC data indicates that both a greater quantity of apo-TC in serum, and TC-R cell membrane expression augmented [^{111}In]AC endocytosis in normal murine tissue and the MDA-MB-231 tumors.

Recently, a novel immunohistochemical staining assay demonstrated that TC-R was overexpressed in MDA-MB-231 tumors and that both TC-R and TC protein expression were markedly elevated in feline mammary carcinomas [31, 32]. The mean staining values for TC-R and TC in feline mammary tumors were 5263 and 5548, respectively, compared to 0.2 and 0.7 in normal peri-tumoral feline mammary tissue. The feline and MDA-MB-231 data

Table 2. *In vivo* uptake of [^{111}In]AC in MDA-MB-231 breast tumors and murine tissue

	DE 0.1 μg [^{111}In]AC	DE 0.5 μg [^{111}In]AC	DE 1.0 μg [^{111}In]AC	PC 2.0 μg AC 2 h	PC 2.0 μg AC 8 h	PC 2.0 μg AC 24 h	PC 40 μg DEX 24 h
Kidney	169.8 ± 20.9	275.2 ± 34.0	875.2 ± 118.2	700.1 ± 71.4	1293.0 ± 224.9	970.3 ± 115.5	1187.5 ± 173.4
Tumor	16.1 ± 0.97	75.7 ± 5.4	102.3 ± 8.9	95.7 ± 7.6	129.9 ± 11.8	145.8 ± 13.3	112.9 ± 11.9
Liver	17.1 ± 1.1	75.7 ± 5.2	70.0 ± 5.5	44.9 ± 3.1	95.7 ± 7.7	78.5 ± 7.2	68.7 ± 5.4
Fat	2.6 ± 0.14	35.8 ± 2.9	28.3 ± 2.1	31.6 ± 2.3	58.6 ± 5.0	40.0 ± 3.6	31.5 ± 2.0
Lung	4.2 ± 0.23	26.3 ± 2.4	32.6 ± 3.1	24.2 ± 1.9	31.6 ± 2.7	28.8 ± 2.6	24.0 ± 1.7
Spleen	5.3 ± 0.29	38.9 ± 3.3	23.2 ± 1.7	16.8 ± 1.2	26.6 ± 2.0	27.9 ± 2.2	30.2 ± 2.8
Heart	2.1 ± 0.09	21.1 ± 1.2	17.4 ± 1.3	15.8 ± 1.2	22.1 ± 1.0	22.2 ± 1.1	22.3 ± 1.2
Muscle	1.1 ± 0.04	10.5 ± 0.5	4.2 ± 0.01	4.1 ± 0.01	12.5 ± 0.7	9.8 ± 0.4	10.5 ± 0.5
Brain	0.34 ± 0.01	3.6 ± 0.12	1.2 ± 0.03	1.3 ± 0.03	2.24 ± 0.02	2.3 ± 0.02	2.3 ± 0.02

Dose escalation (DE). Pulse chase (PC). Rank order of the mean counts/min/mg tissue (CPM/mg) ± the standard deviation (SD) in CPM/mg. The reported CPM/mg and SD values for each tissue type represents the actual counts acquired divided by 1000

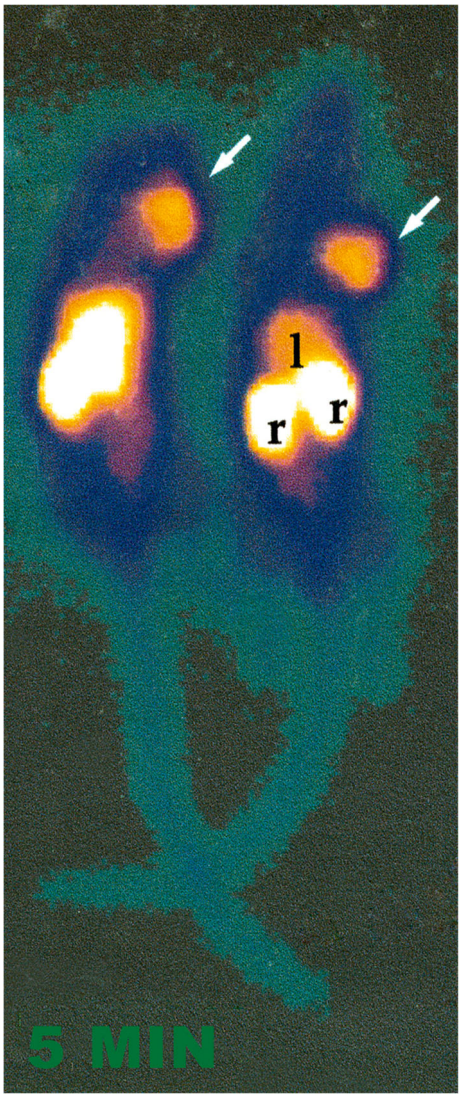

Fig. 5. Planar images of two mice employing a 2-h pulse chase interval between the 2.0 µg AC pulse and 0.5 µg [^{111}In]AC injections. Image acquisition time at 24 h P.I. was 5 min. White arrows indicate [^{111}In]AC uptake in the MDA-MB-231 breast tumors in the cervical soft tissue. Typical liver (l) and renal (r) [^{111}In]AC activity in mice.

indicates that the TC:TC-R pathway was primarily responsible for Cbl endocytosis in human and feline mammary carcinomas.

Cbl Uptake in Breast Tumors Independent of the TC:TC-R Pathway

However, several murine and human studies have indicated that Cbl endocytosis within breast tumors can occur independent of the TC:TC-R pathway. For example, the Megalin (MEG) and CUBAM receptors have both been detected on human breast tumor cell membranes [33]. MEG is a crucial nutritional receptor that promotes cellular proliferation by facilitating the endocytosis of ~50 substrates, including holo-TC, holo-IF, folate, vitamin D, lipoproteins, sterols, hormones, insulin, and sonic hedgehog [34]. MEG can function either independently or in combination with CUBAM when the two receptors are co-localized in tissue. Not surprisingly, MEG and CUBAM receptors are variably expressed throughout embryonic and fetal tissues during development.

The importance of these receptors in supporting cellular proliferation was emphasized when antibodies directed against MEG and CUBAM, but not TC-R, caused fetal demise after their injection into pregnant mice [35]. Correspondingly, murine TC-R knock-out fetuses survived only until birth due to MEG maintaining maternofetal transport of Cbl in the visceral yolk sac and therefore Cbl uptake within fetal brain, spinal cord, and renal tissue *in utero* [36].

In contrast, the expression of MEG and CUBAM receptors in adult humans is essentially limited to tissue barriers that capture and reclaim Cbl. Specifically, CUBAM within the terminal ileum, and MEG-CUBAM or MEG alone in the vascular barriers within the renal proximal tubule, lacrimal/salivary glands, and the choroid plexus. It will therefore be important to investigate if MEG or CUBAM receptor expression occurs on the cell membranes and/or neo-vascularity of breast tumors.

Recently, the increased intracellular concentration of haptocorrin (HC) was reported in multiple tumor cell lines, including within lobular, ductal, and mucinous breast tumor cells [37]. Waibel et al. postulated that an upregulation in the expression of the asialoglycoprotein receptor (ASGP-R), which is responsible for the endocytosis of holo-HC, was the mechanism to affect the increased concentration of HC in tumor cells. Although the overexpression of ASGP-R mRNA was observed in murine fetal and newborn tissues [38], an assay to quantify ASGP-R expression on fetal or tumor cell membranes has yet to be reported.

To determine if the HC:ASGP-R pathway was more effective than the TC:TC-R pathway in imaging Cbl uptake in malignancies, Waibel et al. modified the molecular construct of [^{111}In]AC. By shortening the amide linker covalently bonded to the "b" monocarboxylic acid of the corrin ring and substituting a monoanionic PAMA-ligand for the DTPA chelator, they reported that the new tracer (^{99m}TC(CO)$_3$-[(4-amido-butyl)- pyridine-2-yl-methyl-aminoacetato]-cyanocobalamin) or [^{99m}TC]CC was uniquely bound by HC and IF, but not by TC. The finding was surprising since the selectivity of the transport proteins in binding biochemically active forms of Cbl is IF>TC>>HC [39]. Nevertheless, Waibel et al. reported that the *in vivo* uptake of [^{99m}TC]CC was greater than [^{111}In]CC (not [^{111}In]AC) in a syngeneic murine melanoma model.

Sah et al. subsequently enrolled 10 patients with various known tumors to compare [^{99m}TC]CC SPECT/CT to [^{18}F]FDG PET/CT [40]. In the only breast cancer patient studied, the primary breast tumor had been resected prior to

imaging. Of the multiple [^{18}F]FDG avid metastatic foci of breast cancer depicted by PET/CT, only one lesion was detected by [^{99m}TC]CC SPECT/CT. However, in the remaining six cancer patients investigated, a solitary I.V. bolus of 20 μg or 100 μg of CC was injected 1 h prior to [^{99m}TC]CC administration. Compared to control patients, the serum $T_{1/2}$ clearance of [^{99m}TC]CC decreased from 10 h to 18 min, and the [^{99m}TC]CC T/B ratios on the 4-h SPECT/CT images were reported to have improved.

Future Clinical Imaging of Cbl Uptake in Breast Tumors

The human and murine [^{111}In]AC and [^{99m}TC]CC data suggests that future clinical investigations into imaging Cbl uptake in breast tumors should employ a pulse of AC or CC at 10–20 times the RDA (24 to 48 μg) at 2 or 24 h prior to injecting five times the RDA (12 μg) of a Cbl radiolabeled analog. With the serum $T_{1/2}$ clearance of [^{111}In]AC equaling 7 min, and presuming that a pre-administered pulse of AC decreases [^{111}In]AC background activity in normal breast tissue, the acquisition of WBP or SPECT/CT images could potentially begin routinely at 2 h post-tracer injection. The [^{111}In]AC DE data additionally raises the possibility of simply injecting a solitary 24 μg bolus of [^{111}In]AC, depending upon dosimetry.

Currently no small field of view MBI gamma cameras are capable of imaging [^{111}In]AC uptake in a breast tumor < 0.5 cm. However, two new positron labeled CC analogs and PEM should permit the investigation of Cbl uptake in smaller breast tumors. The positron labeled CC analogs, in contrast to [^{111}In]AC and [^{99m}TC]CC, have a chelator covalently bonded to the 5′-hydroxyl group of the deoxyribose moiety within the phosphate sugar that links the alpha ligand (DMB) to the corrin ring [41, 42]. Both the Cu-64- and Zr-89-labeled cyanocobalamin analogs have imaged tumor xenografts *in vivo*. However, only [^{89}Zr]CC has depicted Cbl uptake in a breast tumor. In the MDA-MB-453 breast tumor xenograft, the greatest uptake of [^{89}Zr]CC occurred at 4 h post I.V. injection.

Cbl Transport and Receptor Proteins in Breast Cancer

The increased serum concentrations of HC and/or TC, reportedly observed in 50–65 % of breast cancer patients, were investigated as potential biomarkers. However, the reported variations in HC and TC expression within breast cancers only underscore the pleiotropic cytogenetic mechanisms remaining to be decrypted. Recently, several genetic aberrations supporting breast tumor growth were discovered to involve the cytogenetic bands encoding the Cbl transport/receptor proteins.

The synthesis of TC in breast tumors was previously posited to be upregulated by *ets* transcription factors and a *c-myc* protein binding to specialized nucleic acid base motifs in the promoter region of the TC gene (TCN2) on chromosome 22q12.2 [43]. More recently, the amplification of the leukemia inhibitory factor (LIF) gene located on 22q.12.2 was discovered to promote the tumorigenesis and metastasis of breast cancer through the AKT-mTOR pathway [44].

Correspondingly, human lactating breast tissue normally upregulates HC production ~100–400 times to insure the delivery of Cbl to nursing newborns [45]. Although the cytogenetic mechanisms triggering the overexpression of HC in maternal lactating breast tissue and malignant breast tumor cells remain to be elucidated, the CTNND1 gene on 11q12.1, where HC (TCN1) and IF (GIF) genes are encoded, is frequently modified in biologically aggressive breast cancers [46].

Finally, on the cytogenetic bands encoding the Cbl receptor protein genes: TC-R (CD320) on 19p13.2, MEG (LRP2) on 2q31.1, cubilin (CUBN) on 10p13, amnionless (AMN) on 14q32.32, and ASGP-R (ASGR1 and ASGR2) on 17p13.1, are foci of gene amplification or mutations that support breast tumor progression, for example, the amplification of DNMT1 on 19p13.2 [47], PDK1 on 2q31.1 [48], CAMK1D on 10p13 [49], and AKT1 on 14q32.32 [50] and mutations of TP53 on 17p13.1 [51]. Intriguingly, with the concentration of sCD320 increasing in urine and serum during pregnancy, it suggests that the protein fragment may be a biomarker for cellular proliferation [52].

Conclusion

The uptake of Cbl in malignant breast tumors can be clinically imaged and biochemically enhanced. Further investigation into targeting the Cbl metabolic pathway in breast tumors is warranted and could potentially uncover novel theragnostic targets.

Acknowledgements. Dr. H.P.C. Hogenkamp synthesized the AC analog. Dr. Douglas A Collins radiolabeled the AC analog. Linda M. Thorson CNMT performed the [^{111}In]AC plasma and urine clearance assays. Timothy J. Hardyman CNMT acquired the WB/SPECT images and calculated the [^{111}In]AC T/B ratios. Rebecca M. Wilson completed the murine biodistribution studies. Rebecca A. Thompson and Michelle W. Andersen created the illustrations. Rose M. Busta facilitated manuscript production.

Compliance with Ethical Standards

Conflict of Interest

Dr. Douglas A Collins and Dr. H.P.C. Hogenkamp have intellectual property related to the radiolabeling of cobalamin that is jointly held by Mayo Clinic and the University of Minnesota. The Cbl research has been funded by the Mayo Foundation and the University of Minnesota.

References

1. Plevritis SK, Munoz D, Kurian AW et al (2017) Association of Screening and Treatment with Breast Cancer Mortality by molecular subtype in US women, 2000-2012. J Am Med Assoc 319:154–164
2. Iqbal J, Ginsburg O, Rochon PA, Sun P, Narod SA (2015) Differences in breast cancer stage at diagnosis and cancer-specific survival by race and ethnicity in the United States. J Am Med Assoc 313:165–173
3. Boyd NF, Guo H, Martin LJ, Sun L, Stone J, Fishell E, Jong RA, Hislop G, Chiarelli A, Minkin S, Yaffe MJ (2007) Mammographic density and the risk in detection of breast cancer. N Engl J Med 356:227–236
4. Rhodes D, O'Connor M, Phillips S et al (2005) Molecular breast imaging: a new technique using technetium Tc 99m scintimammography to detect small tumors of the breast. Mayo Clin Proc 80:24–30
5. Hsu DFC, Freese DL, Levin CS (2016) Breast-dedicated radionuclide imaging systems. J Nucl Med 57:40S–45S
6. Van Es SC, Venema CM, Glaudemans AWJM et al (2016) Translation of new molecular imaging approaches to the clinical setting: bridging the gap to implementation. J Nucl Med 57:96S–104S
7. Shermis RB, Wilson KD, Doyle MT, Martin TS, Merryman D, Kudrolli H, Brenner RJ (2016) Supplemental breast cancer screening with molecular breast imaging for women with dense breast tissue. AJR 207:450–457
8. Ulaner GA, Riedl CC, Dickler MN, Jhaveri K, Pandit-Taskar N, Weber W (2016) Molecular imaging of biomarkers in breast cancer. J Nucl Med 57:53S–59S
9. Wooley DW (1953) Evidence for the synthesis of vitamin B12 by spontaneous mammary tumors. Proc Nat Acad Sci USA 39:6–18
10. Carmel R, Eisenberg L (1977) Serum vitamin B_{12} and transcobalamin abnormalities in patients with cancer. Cancer 40:1348–1353
11. Rachmilewitz B, Rachilewitz M (1981) Serum transcobalamin-II levels in breast-carcinoma patients. Isr J Med Sci 17:874–878
12. Flohd H, Ullberg S (1968) Accumulation of labelled vitamin B_{12} in some transplanted tumours. Int J Cancer 3:694–699
13. Quadros EV, Sequeira JM (2013) Cellular update of cobalamin: Transcobalamin and the TCbIR/*CD320* receptor. Biochemie 95:1008–1018
14. Quadros EV, Rothenberg SP, Polu S (1988) A specific radioimmunoassay for 5'deoxyadenosylcobalamin in serum. Br J Haematol 69:551–557
15. Brazenas GR, Bartkeviciene VV, Aleksiene AM et al (1979) On some properties of the effect and metabolism of different cobalamins in tumor-bearing rats. In: Zagalak B, Friedrich W (eds) Vitamin B_{12}. Walter de Gruyter, Berlin, pp 1113–1118
16. Hall CA, Colligan PD, Begley JA (1987) Cyclic activity of the receptors of cobalamin bound to transocbalamin II. J Cellular Physiol 133:187–191
17. Collins DA, Hogenkamp HPC (1997) Transcobalamin II receptor imaging via radiolabeled diethylenetriaminepentaacetate cobalamin analogs. J Nucl Med 38:717–723
18. Hogenkamp HPC, Collins DA, Grissom CB, West FG (1999) Diagnostic and therapeutic analogues of cobalamin. In: Banerjee R (ed) Chemistry and biochemistry of B12. John Wiley & sons, New York, pp 385–410
19. Cruz R, Steyn P, Collins D, Powers B, Urigh J (2011) Radiography, ^{99m}Tc-HDP, and ^{111}In labeled vitamin B_{12} SPECT of canine osteosarcoma: a comparative study. J Am Animal Hosp Assoc 47:229–235
20. Collins DA, Hogenkamp HPC, Gebhard MW (1999) Tumor imaging via indium 111-labeled DTPA-adenosylcobalamin. Mayo Clin Proc 74:687–691
21. Collins DA, Hogenkamp HPC, O'Connor MK, Naylor S, Benson LM, Hardyman TJ, Thorson LM (2000) Biodistribution of radiolabeled adenosylcobalamin in patients diagnosed with various malignancies. Mayo Clin Proc 75:568–580
22. Greipp PT, Collins DA, Russell SJ, et al. (2006) In-111 DAC is a novel technique to image multiple myeloma (abstract 3488). Blood 108 (11 Part 1): 944 a
23. Benard F, Turcotte E (2005) Imaging in breast cancer: single-photon computed tomography and positron-emission tomography. Breast Cancer Res 7:153–162
24. Stanton SE, Eary JF, Marzbani A, Mankoff D et al (2016) Concurrent SPECT/PET-CT imaging as a method for tracking adoptively transferred T-cells *in vivo*. J Immunother Cancer 4:27
25. Carmel R, Watkins D, Rosenblatt DS (2015) Megaloblastic Anemia. In: Orkin SH, Fisher DE, Ginsburg D et al (eds) Nathan and Oski's hematology and oncology of infancy and childhood, 8th edn. Saunders, Philadelphia, pp 308–343
26. Frost DV, Fricke HH, Spruth HC (1949) Rat growth assay for vitamin B12. Proc Soc Exp Biol Med 72:102–106
27. Arendt JFB, Nexo E (2012) Cobalamin related parameters and disease patterns in patients with increased serum cobalamin levels. PLoS One 7:e45979
28. Lildballe DL, Mutti E, Birn H, Nexo E (2012) Maximal load of the vitamin B12 transport system: a study on mice treated for four weeks with high-dose vitamin B12 or cobinamide. PLoS One 7:e46657
29. Donaldson RM, rand M, Serfilippi D (1977) Changes in circulating transcobalamin II after injection of cyanocobalamin. N Engl J Med 296:1427–1430
30. Granat M, Rachmilewitz B, Mor-Yosef S et al (1983) Effect of dexamethasone on serum transcobalamin II concentration in women undergoing pelvic surgery. Eur J Clin Pharmacol 25:6221–6624
31. Sysel AM, Valli VE, Nagle RB, Bauer JA (2013) Immunohistochemical quantification of the vitamin B12 transport protein (TCII), cell surface receptor (TCII-R) and Ki-67 in human tumor xenografts. Anticancer Res 33:4203–4212
32. Sysel AM, Valli VE, Bauer JA (2014) Immunohistochemical quantification of the cobalamin transport protein, cell surface receptor and Ki-67 in naturally occurring canine and feline malignant tumors and in adjacent normal tissues. Oncotarget 6:2331–2348
33. Chlon TM, Taffany DA, Welsh J, Rowling MJ (2008) Retinoids module expression of the endocytic partners megalin, cubilin, and disabled-2 and uptake of vitamin D-binding protein in human mammary cells. Nutrition 138:1323–1328
34. Christensen EI, Birn H (2002) Megalin and cubulin: multifunctional endocytic receptors. Nature 3:258–268
35. Kozyrak R, Gofflot F (2007) Multiligand endocytosis and congenital defects: roles of cubilin, megalin and amnionless. Curr Pharm Des 13:3038–3046
36. Arora K, Sequeira J, Quadros E (2017) Maternofetal transport of vitamin B12: role of TCblR/CD320 and megalin. FASEB 31:3098–3106
37. Waibel T, Treichler H, Schaefer NG et al (2008) New derivatives of vitamin B12 show preferential targeting of tumors. Cancer Res 68:2904–2911
38. Mu J-Z, Tang L-H, Alpers DH (1993) Asialoglycoprotein receptor mRNAs are expressed in most extrahepatic rat tissues during development. Am J Phys 264:G752–G762
39. Wuerges J, Geremia S, Randaccio L (2007) Structural study on ligand specificity of human vitamin B12 transporters. Biochem J 403:431–440
40. Sah B-R, Schibli R, Waibel R et al (2014) Tumor imaging in patients with advanced tumors using a new ^{99m}Tc-radiolabeled vitamin B12 derivative. J Nucl Med 55:43:43–43:49
41. Ikotun OF, Marquez BV, Fazen CH et al (2014) Investigation of a vitamin B12 conjugate as a PET imaging probe. ChemMedChem 9:1244–1251
42. Akhila N, Kuda-Wedagedara W, Workinger JL et al (2017) ^{89}Zr-cobalamin PET tracer: synthesis, cellular uptake, and use for tumor imaging. ACS Omega 2:6314–6320
43. Regec A, Quadros EV, Platica O, Rothenberg SP (1995) The cloning and characterization of the human transcobalamin II gene. Blood 85:2711–2719
44. Li X, Yang Q, Yu H, Wu L, Zhao Y, Zhang C, Yue X, Liu Z, Wu H, Haffty BG, Feng Z, Hu W (2014) LIF promotes tumorigenesis and metastasis of breast cancer through the AKT-mTOR pathway. Oncotarget 5:788–801
45. Lildballe Dl HTF, Allen LH, Nexo E (2009) High concentrations of haptocorrin interfere with routine measurement of cobalamins in human serum and milk. A problem and its solution. Clin Chem Lab Med 47:182–187
46. Schackmann R, Klarenbeek S, Vlug E et al (2013) Loss of p120-catenin induces metastatic progression of breast cancer by inducing Anoikis resistance and augmenting growth factor receptor signaling. Cancer Res 73:4937–4949

47. Pathania R, Ramachandran S, Elangovan S, Padia R, Yang P, Cinghu S, Veeranan-Karmegam R, Arjunan P, Gnana-Prakasam JP, Sadanand F, Pei L, Chang CS, Choi JH, Shi H, Manicassamy S, Prasad PD, Sharma S, Ganapathy V, Jothi R, Thangaraju M (2015) DNMT1 is essential for mammary and cancer stem cell maintenance and tumorigenesis. Nat Commun 6:6910
48. Du J, Yang M, Chen S et al (2016) PDK1 promotes tumor growth and metastasis in a spontaneous breast cancer model. Oncogene 35:3314–3323
49. Bergamaschi A, Kim YH, Kwei KA, la Choi Y, Bocanegra M, Langerød A, Han W, Noh DY, Huntsman DG, Jeffrey SS, Børresen-Dale AL, Pollack JR (2008) *CAMK1D* amplification implicated in epithelial-mesenchymal transition in basal-like breast cancer. Mol Oncol 2:327–339
50. Riggio M, Perrone MC, Polo ML et al (2017) AKT1 and AKT2 isoforms play distinct roles during breast cancer progression through the regulation of specific downstream proteins. Nature: Scientific Reports 7:44244
51. Liu Y, Chen C, Xu Z, Scuoppo C, Rillahan CD, Gao J, Spitzer B, Bosbach B, Kastenhuber ER, Baslan T, Ackermann S, Cheng L, Wang Q, Niu T, Schultz N, Levine RL, Mills AA, Lowe SW (2016) Deletions linked to TP53 loss drive cancer through p53-independent mechanisms. Nature 531:471–475
52. Abuyaman O, Andreasen BH, Kronberg C et al (2013) The soluble receptor for vitamin B12 uptake (sCD320) increases during pregnancy and occurs in higher concentration in urine than in serum. PLoS One 8:e73110